AMERICAN SOCIETY FOR MICROBIOLOGY | Journal of Bacteriology®

RESEARCH ARTICLE

CpxR-Dependent Thermoregulation of *Serratia marcescens* PrtA Metalloprotease Expression and Its Contribution to Bacterial Biofilm Formation

Roberto E. Bruna,[a] María Victoria Molino,[a] Martina Lazzaro,[a] Javier F. Mariscotti,[a] Eleonora García Véscovi[a]

[a]Instituto de Biología Molecular y Celular de Rosario, Consejo Nacional de Investigaciones Científicas y Tecnológicas, Universidad Nacional de Rosario, Rosario, Santa Fe, Argentina

ABSTRACT PrtA is the major secreted metalloprotease of *Serratia marcescens*. Previous reports implicate PrtA in the pathogenic capacity of this bacterium. PrtA is also clinically used as a potent analgesic and anti-inflammatory drug, and its catalytic properties attract industrial interest. Comparatively, there is scarce knowledge about the mechanisms that physiologically govern PrtA expression in *Serratia*. In this work, we demonstrate that PrtA production is derepressed when the bacterial growth temperature decreases from 37°C to 30°C. We show that this thermoregulation occurs at the transcriptional level. We determined that upstream of *prtA*, there is a conserved motif that is directly recognized by the CpxR transcriptional regulator. This feature is found along *Serratia* strains irrespective of their isolation source, suggesting an evolutionary conservation of CpxR-dependent regulation of PrtA expression. We found that in *S. marcescens*, the CpxAR system is more active at 37°C than at 30°C. In good agreement with these results, in a *cpxR* mutant background, *prtA* is derepressed at 37°C, while overexpression of the NlpE lipoprotein, a well-known CpxAR-inducing condition, inhibits PrtA expression, suggesting that the levels of the activated form of CpxR are increased at 37°C over those at 30°C. In addition, we establish that PrtA is involved in the ability of *S. marcescens* to develop biofilm. In accordance, CpxR influences the biofilm phenotype only when bacteria are grown at 37°C. In sum, our findings shed light on regulatory mechanisms that fine-tune PrtA expression and reveal a novel role for PrtA in the lifestyle of *S. marcescens*.

IMPORTANCE We demonstrate that *S. marcescens* metalloprotease PrtA expression is transcriptionally thermoregulated. While strongly activated below 30°C, its expression is downregulated at 37°C. We found that in *S. marcescens*, the CpxAR signal transduction system, which responds to envelope stress and bacterial surface adhesion, is activated at 37°C and able to downregulate PrtA expression by direct interaction of CpxR with a binding motif located upstream of the *prtA* gene. Moreover, we reveal that PrtA expression favors the ability of *S. marcescens* to develop biofilm, irrespective of the bacterial growth temperature. In this context, thermoregulation along with a highly conserved CpxR-dependent modulation mechanism gives clues about the relevance of PrtA as a factor implicated in the persistence of *S. marcescens* on abiotic surfaces and in bacterial host colonization capacity.

KEYWORDS *Serratia*, PrtA, CpxAR, TCS, biofilm, CpxR, thermoregulation, serralysin

Serratia marcescens belongs to the *Enterobacteriaceae* family and can be isolated from a wide variety of environmental niches, ranging from water and soil to air. In addition to its environmental ubiquity, *S. marcescens* is an emergent health-threatening nosocomial pathogen. In recent years, outbreaks of multidrug-resistant strains and high incidence in intensive and neonatal care units have increasingly been reported (1–3). The World Health Organization recently declared *S. marcescens*, together with other

Received 4 January 2018 **Accepted** 20 January 2018

Accepted manuscript posted online 29 January 2018

Citation Bruna RE, Molino MV, Lazzaro M, Mariscotti JF, García Véscovi E. 2018. CpxR-dependent thermoregulation of *Serratia marcescens* PrtA metalloprotease expression and its contribution to bacterial biofilm formation. J Bacteriol 200:e00006-18. https://doi.org/10.1128/JB.00006-18.

Editor Conrad W. Mullineaux, Queen Mary University of London

Address correspondence to Eleonora García Véscovi, garciavescovi@ibr-conicet.gov.ar.

enterobacteria, a research priority target to develop alternative antimicrobial strategies given the high frequency of carbapenem-resistant clinical isolates (4). In a recent work, Hoarau et al. (5) also identified *S. marcescens* as one of the three most abundant microbial species that colonize the dysbiotic gut of Crohn's disease patients, in detriment to beneficial bacteria. *S. marcescens* can also develop either symbiotic or pathogenic interactions with plants and insects (6).

The ability of *S. marcescens* to adapt to and survive in both hostile and changing environments also relates to the bacterial capacity to express a wide range of secreted enzymes, including lipases, phospholipases, chitinases, proteases, and nucleases (6). Typically, the catalytic action of secreted effectors allows bacteria to perform vital tasks outside or within a host, such as conversion of environmental compounds in usable nutrient sources, adherence to surfaces, and breaching of host protective barriers along colonization pathways or manipulation of intracellular traffic pathways within invaded cells. The expression of these multiple effectors needs to be coordinated at the right time and in the right place to allow bacteria to thrive and shift between different lifestyles.

PrtA, also named serralysin or PrtS (7), is a 50.2-kDa repeats-in-toxin (RTX) alkaline zinc metalloprotease that has been well characterized structurally (8) and was shown to depend on the type I LipBCD system for secretion to the extracellular milieu (9, 10). Similarly to proteases that belong to the serralysin family in other bacteria, such as *Photorhabdus*, *Erwinia*, or *Pseudomonas*, *S. marcescens* PrtA has been implicated in cytotoxicity, immunomodulation, or virulence traits using different experimental models, including nematodes, insects, and mice (11–17). In addition, the potential application of the enzymatic properties of PrtA, for instance, as a detergent additive, has attracted industrial interest, and different purification strategies and the optimization of its catalytic activity have been reported (15, 18–22). In several countries, purified serralysins are also commercially available as potent analgesic and anti-inflammatory drugs (23).

One of the most conspicuous mechanisms that pathogenic bacteria display to tightly regulate the expression of bacterial effectors in response to either extra- or intrahost challenges are the so-called two-component systems (TCS). In these signal transduction systems, the activation of a sensor histidine kinase leads to autophosphorylation followed by transfer of the phosphoryl group to a cognate response regulator in an aspartate residue. CpxAR is a canonical TCS, broadly conserved among many pathogenic and nonpathogenic bacteria. In most of these organisms, CpxAR regulates gene expression to counteract stressful conditions that menace bacterial envelope intactness. CpxA, a histidine kinase, can detect a variety of stimuli that range from pH alterations and overexpression of envelope proteins (such as NlpE or pilus subunits) to toxic concentrations of metal ions (24–27). Upon phosphate transfer from the CpxA sensor, the phosphorylated cognate response regulator CpxR generates the output response by driving the transcriptional expression of numerous genes. The Cpx regulon comprises both evolutionarily conserved genes, such as those for the protease/chaperone DegP (25), the disulfide bond oxidoreductase DsbA (24), and CpxP, which functions as both a chaperone and a repressor of the Cpx response (28), as well as species-specific genes involved in diverse phenotypes, including antibiotic resistance, motility, and biofilm formation (29, 30).

Biofilm is an orchestrated collective form of bacterial life that relies on the timely production of an intricate extracellular mesh that structurally and functionally supports its formation. This extracellular matrix can be composed of self-produced exopolysaccharides, proteins, lipids, DNA, and bacterial appendices such as fimbria and flagella. Previous work has shown that *S. marcescens* is able to develop biofilm associated with either biotic or abiotic surfaces (31–34). This ability is associated with the capacity of *Serratia* to colonize and persist in medical devices, such as catheters or prostheses (35), and to enhance bacterial resistance to antibiotics (36).

In this work, we characterized regulatory aspects that govern *S. marcescens* PrtA production. We found that PrtA expression is subject to transcriptional regulatory

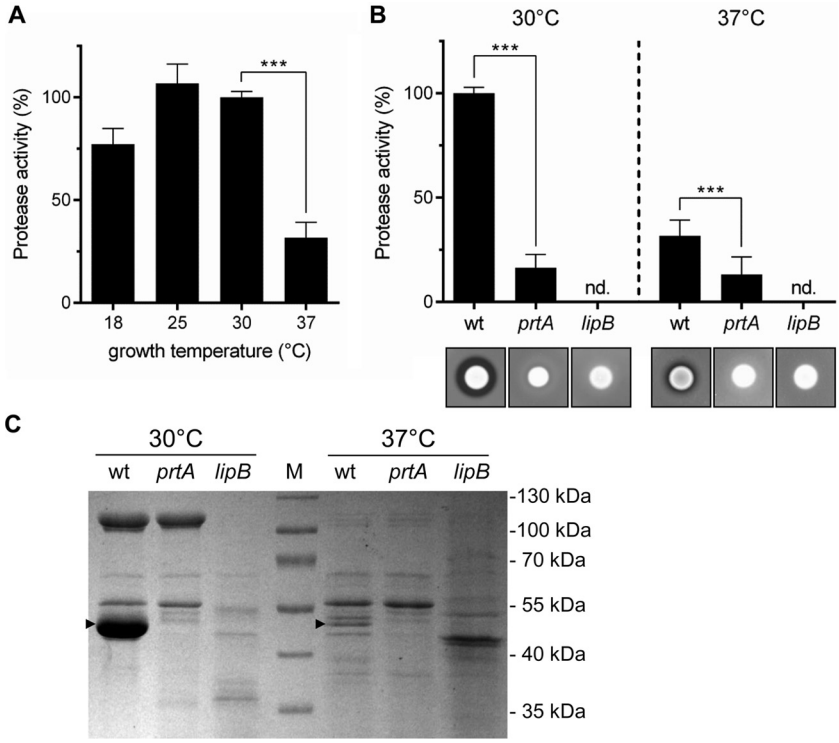

FIG 1 Dependence of *S. marcescens* RM66262 PrtA on the bacterial growth temperature. (A) Secreted protease activity from the *S. marcescens* wild-type strain grown in LB medium for 16 h at the indicated temperatures. (B) Secreted protease activities from wild-type, *prtA*, and *lipB* strains grown for 16 h at the indicated temperatures. Below the graph, representative LB agar-skim milk plate images show protease degradation halos for each strain. For both panels A and B, protease activity was measured by the azocaseinase assay. Activity results are expressed as percentages relative to the value of the wild-type strain grown at 30°C. Means ± SDs from three independent experiments are shown. Significant differences in activity by unpaired *t* test between the indicated strains are shown as follows: ***, $P < 0.001$, and nd., not detected. (C) SDS-PAGE analysis of extracellular proteins from the wild-type, *prtA*, and *lipB* strains grown in LB medium for 16 h at 30°C or 37°C, as indicated. The arrowheads indicate the positions of the PrtA protein. Molecular mass standards are indicated to the right.

mechanisms that involve the bacterial growth temperature and the action of the Cpx signal transduction system. In addition, we reveal that PrtA expression influences the ability of *Serratia* to develop a mature biofilm.

RESULTS AND DISCUSSION

The expression of PrtA, the major *S. marcescens* secreted protease, is thermoregulated at the transcriptional level. Phenotypes influenced by temperature have been previously observed in *Serratia*, such as flagellum-dependent swimming or swarming motility (37, 38), the generation of outer membrane vesicles (OMVs) (39), or the production of metalloproteases and serine proteases in certain strains, such as *Serratia* sp. strain SCBI (38, 40). To examine whether exoprotease expression is affected by bacterial growth temperature in *S. marcescens* clinical strain RM66262 (41), we first determined total proteolytic activity in the culture supernatant after growing *S. marcescens* at different temperatures in the range of 18 to 37°C. Proteolytic activity was quantified in *S. marcescens* culture supernatants by using azocasein as the substrate, as described previously (42). As shown in Fig. 1A, a 68.3% decrease of total proteolytic activity was observed when bacterial growth temperature was increased from 30°C to 37°C. According to previous work, PrtA is responsible for the main proteolytic activity that *S. marcescens* secretes into the culture medium (43). Therefore, we constructed a *prtA* null mutant and evaluated protease activity in this strain. As shown in Fig. 1B, in comparison with wild-type (wt) levels, proteolytic activity dramatically decreased in the mutant strain at the two temperatures tested (83.6% at 30°C and 58.7% at 37°C).

Neither the wild-type nor the *prtA* strain showed alterations in growth capacity at the tested temperatures (data not shown). The decreased proteolytic activity of the *prtA* strain and the observed modulation by temperature were also qualitatively detected by the width of clear halos around the colony that result from proteolytic activity when strains are grown in LB agar-skim milk plates (Fig. 1B). The relative abundance of PrtA among proteins secreted by *Serratia* and its temperature-dependent production were examined by SDS-PAGE analysis of the bacterial culture supernatant (Fig. 1C). The identity of the protein labeled PrtA was confirmed by excision of the band from the polyacrylamide gel, followed by enzymatic digestion with trypsin and tandem mass spectrometry (MS/MS), as detailed in Materials and Methods. The absence of PrtA expression in the *prtA* mutant strain could be also observed by SDS-PAGE analysis at both temperatures tested (Fig. 1C). The remnant protease activity detected in the *prtA* background (Fig. 1B) can be attributed to the expression of other proteases. Indeed, when we performed an *in silico* analysis of the *S. marcescens* RM66262 genome, in addition to *prtA*, we found that it includes *slpC*, *slpD*, and *slpE* homologues (44, 45), all of them containing the N-terminal HEXXHXXGXXH domain and RTX repeats, the main features of serralysin family proteins.

It has been previously shown that the LipBCD type I secretion system mediates the extracellular export of PrtA (9). As shown in Fig. 1B, inactivation of *lipB* resulted in the abrogation of secreted proteolytic activity when bacteria were grown either at 30°C or at 37°C. As expected, the absence of the PrtA band was observed in the *lipB* strain culture supernatant (Fig. 1C). These results indicate that all detectable extracellular proteolytic activities of *S. marcescens* RM66262 strain rely on a functional LipBCD type I secretion system for their secretion.

At either 30°C or 37°C, complementation of the *prtA* mutant defect in protease secretion was achieved by expression of *prtA* under the control of a constitutive promoter from the pBB2::*prtA* plasmid (Fig. 2A). Temperature dependence on secreted protease activity was still observed in the *prtA* complemented strain. In order to further analyze this result, we determined *prtA* transcriptional levels by quantitative real-time PCR (qRT-PCR). As shown in Fig. 2B, *prtA* transcript levels were 29-fold higher at 30°C versus 37°C in the wild-type strain, indicating that thermoregulation occurs at the transcriptional level. In contrast to secreted protease activity results, the complemented *prtA*/pBB2::*prtA* strain reached the same transcriptional expression values irrespective of the bacterial growth temperature. These results suggest that (i) the difference in steady-state levels of *prtA* transcript between 30°C and 37°C is not related to differential, temperature-dependent mRNA stability, as equivalent levels were measured from the constitutive pBB2::*prtA* expression plasmid, and (ii) the failure to lose thermal modulation of the secreted activity by constitutive expression of *prtA* indicates additional thermoregulated factors that influence PrtA expression.

To further examine the mechanism that underlies thermoregulation of PrtA expression, we constructed the P*prtA-gfp* reporter plasmid harboring the *gfp* gene, which encodes green fluorescent protein (GFP) under the transcriptional control of the *prtA* promoter region (443 bp upstream of the translational ATG start codon of *prtA*). As shown in Fig. 2C, transcriptional activity was 246% higher when bacteria were grown at 30°C versus 37°C. This result indicates that a thermoregulatory mechanism targets the *prtA* promoter region. To analyze if expression of the dedicated transporter LipBCD was also affected by growth temperature at the transcriptional level, we measured fluorescence from a P*lipBCD-gfp* transcriptional reporter, which harbors 500 bp corresponding to the putative *lipBCD* promoter region fused to the *gfp* gene. We found that in the wild-type strain, after 16 h of growth at 30°C, fluorescence reached a value 31% higher than the one obtained at 37°C (Fig. 2C).

Therefore, we can infer that increased PrtA expression at low temperatures needs to be coordinated with an enhanced secretion capacity, achieved by higher levels of expression of the Lip transporter system. This result also indicates that LipBCD expression would differentially limit PrtA secretion at 30°C or 37°C and explains why even when the transcript is constitutively expressed in the *prtA*/pBB2::*prtA* complemented

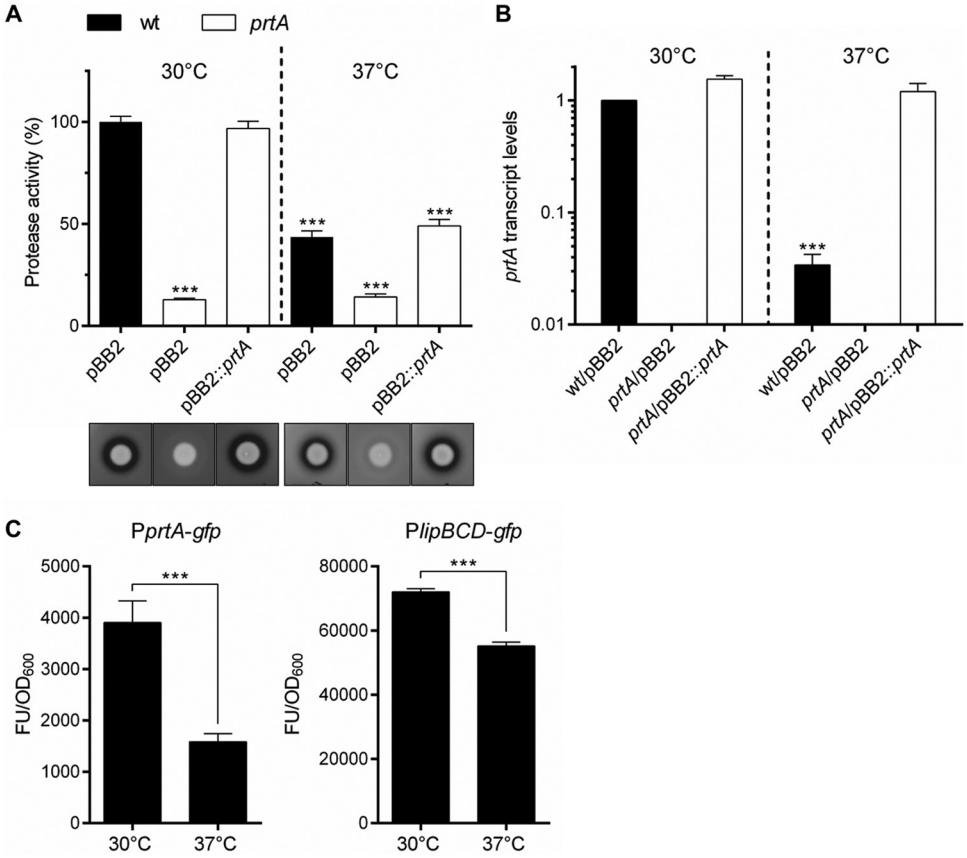

FIG 2 (A) Complementation of the *prtA* mutant by in *trans* expression of *prtA*. Protease activity was measured by the azocaseinase assay. The results of proteolytic activity are expressed as percentages relative to the value of the wt/pBB2 strain grown in LB for 16 h at 30°C. Below the graph, representative LB agar-skim milk plate images show protease degradation halos for each strain. Means ± SDs from three independent experiments are shown. Significant differences in activity relative to the wt/pBB2 strain grown at 30°C calculated by one-way analysis of variance (ANOVA) with Bonferroni's multiple-comparison test are indicated as follows: ***, $P < 0.001$. (B) qRT-PCR analysis of *prtA* transcriptional expression. The value obtained for the wt/pBB2 strain grown in LB medium for 16 h at 30°C was taken as the reference value. mRNA levels were normalized to 16S rRNA expression. Relative expression was calculated using the $2^{-\Delta\Delta CT}$ method. Means ± SDs from three independent experiments are shown. Significant difference versus reference value calculated by paired *t* test is indicated as follows: ***, $P < 0.001$. (C) Transcriptional expression of *prtA* and *lipBCD*. Bacteria were grown for 16 h in LB medium at the indicated temperatures. Transcriptional activity was calculated as the ratio of GFP fluorescence and OD_{600} (FU/OD_{600}) measured from the wild-type strain carrying the P*prtA-gfp* or P*lipBCD-gfp* reporter plasmids. Means ± SDs from three independent experiments are shown. Significant differences between growth temperatures calculated by unpaired *t* test are indicated as follows: ***, $P < 0.001$.

strain, we still observe a temperature-dependent effect in secreted protease activity levels. Overall, these results show that expression of PrtA, which is responsible for the major secreted proteolytic activity in *S. marcescens*, is modulated by the bacterial growth temperature at the transcriptional level.

CpxR directly binds to a conserved motif within the *prtA* promoter. To gain further insight into the mechanism that underlies *prtA* regulated expression, we performed a bioinformatic search in the putative promoter region of *prtA*, comprising 443 bp upstream of the translational ATG. The use of the MEME/FIMO (46, 47) predictive tools showed a putative CpxR-binding site 216 bp upstream of the *prtA* ATG translational initiation codon. This CpxR-binding sequence showed 14 out of 16 conserved bases in comparison with the consensus motif constructed by the search engine using a series of previously identified promoter regions that contain CpxR bona fide recognition sequences (Fig. 3). Extending the search to annotated *Serratia marcescens* genomes, we found that the CpxR-binding motif was highly conserved in all examined *prtA* promoter regions irrespective of the clinical, enthomopathogenic, or environmen-

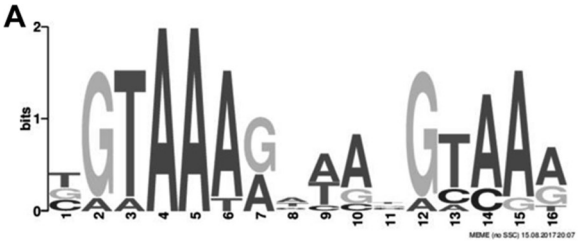

B

Serratia marcescens* RM66262	TCATTTGTTT TGTAAAGAAGCCAAAA AAGCAGCATA...206 bp ATG
Serratia marcescens* SMB2099	TCATTTGTTT TGTAAAGAAGCCAAAA AAGCAGCATA...206 bp ATG
Serratia marcescens* UNAM836	TCATTTGTTT TGTAAAGAAGCCAAAA AAGCAGCATA...206 bp ATG
Serratia marcescens* SM39	TCATTTGTTT TGTAAAGAAGCCAAAA AAGCAGCATA...206 bp ATG
Serratia marcescens* U36365	TCATTTGTTT TGTAAATAAGCCTAAA AAGCAGCATA...206 bp ATG
Serratia marcescens* CAV1492	TCATTTGTTT TGTAAATAAACCTAAA AAGCAGCATA...206 bp ATG
***Serratia marcescens subs. marcescens* Db11•**	TCGTTTGCTT TGTAAAGAAGCCTAAA AAGCAGCATA...206 bp ATG
***Serratia marcescens* WW4◦**	TCATTTGTTT TGTAAATAAGCCTAAA AAGCAGCATA...206 bp ATG
***Serratia sp.* Fs14◦**	TCATTTGCTT TGTAAAGAACTCTAAA AAGCAGCATA...206 bp ATG
***Serratia liquefaciens* ATCC 27592◦**	TCATTAATAT TGTAAAGAACGCAAAA AACCAGCATA...206 bp ATG
Serratia proteamaculans* 568	TCATTTAGAT TGTAAGTATCGCCAAA AACCAGCATA...206 bp ATG

FIG 3 *In silico* analysis of CpxR-binding site. (A) The logo shows the DNA consensus motif for the CpxR-binding site obtained by MEME/FIMO bioinformatics tools. (B) CpxR-binding motif is conserved in *Serratia prtA* promoter regions. The predicted CpxR-binding site sequence in the putative promoter region of *S. marcescens* RM66262 *prtA* is underlined. DNA sequences deposited in the NCBI database under the following numbers were used for the analysis of putative CpxR-binding sites within the *prtA* promoter region in *Serratia* strains: NZ_JWLO00000000.1 (*S. marcescens* RM66262), NZ_HG738868.1 (*S. marcescens* SMB2099), NZ_CP012685.1 (*S. marcescens* UNAM836), NZ_AP013063.1 (*S. marcescens* SM39), NZ_CP016032.1 (*S. marcescens* U36365), NZ_CP011642.1 (*S. marcescens* CAV1492), NZ_HG326223.1 (*Serratia marcescens* subsp. *marcescens* Db11), NC_020211.1 (*S. marcescens* WW4), NZ_CP005927.1 (*Serratia* sp. FS14), NC_021741.1 (*Serratia liquefaciens* ATCC 27592), and NC_009832.1 (*Serratia proteamaculans* 568). The type of isolate is indicated as follows: asterisk, clinical; solid dot, enthomopathogenic; open dot, environmental.

tal origin of the isolate, and it was even detected in the *Serratia liquefaciens* and *Serratia proteamaculans* genomes (Fig. 3B).

To assess whether CpxR is able to directly interact with the putative regulatory region upstream of *prtA*, electrophoretic mobility shift (EMSA) and DNase I footprinting assays were performed. For EMSA, a PCR-amplified fragment derived from the *prtA* promoter region encompassing 443 bp upstream of the translational ATG and purified 6×His-tagged CpxR (CpxR-6×His) protein were used. Phosphorylation of CpxR was achieved by use of acetyl phosphate as a phosphoryl donor. A retarded band was detected when 20 pmol of phosphorylated CpxR was used (Fig. 4A), indicating that, as predicted, CpxR is able to recognize a CpxR-binding motif within the fragment. A 10- to 162-fold excess of competing nonspecific *nucA* DNA fragment (a 436-bp DNA region that codes for the *S. marcescens* NucA nuclease) did not affect the interaction (Fig. 4A, left), while the shifted band was progressively lost when increasing amounts of unlabeled *prtA* promoter fragment were included in the mixture (Fig. 4A, right), indicating that the interaction of CpxR with the *prtA* promoter region is specific. To determine whether CpxR phosphorylation status affected the capacity for DNA binding, we compared the mobility shift abilities of CpxR when it was preincubated in the absence and presence of acetyl phosphate. At least 10 pmol of nonphosphorylated CpxR was required to shift the mobility of the DNA probe, while 5 pmol of the phosphorylated form was enough to exert the effect, indicating that phosphorylation enhances CpxR binding affinity for its target sequence in the DNA (Fig. 4B). For the DNase I protection assay, CpxR-6×His previously incubated with acetyl phosphate and labeled DNA fragments containing either coding or noncoding sequences 443 bp upstream of the translational ATG start of *prtA* were used. As shown in Fig. 4C, CpxR-6×His protected an overlapping region from nucleotides −216 to −241 relative

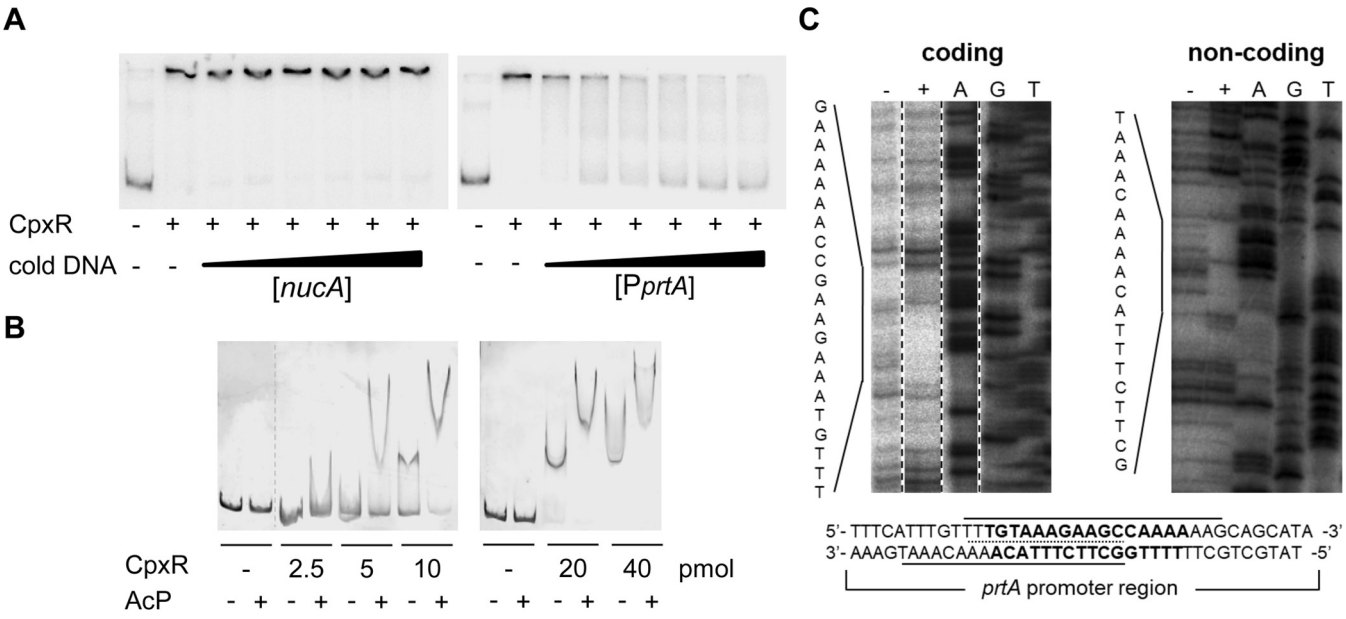

FIG 4 CpxR interaction with a CpxR-binding motif within the *S. marcescens prtA* promoter region. (A) Electrophoretic mobility shift assays (EMSAs) were performed using 20 pmol of purified CpxR-6×His. Target DNA was a ^{32}P-labeled PCR fragment that included the *prtA* promoter region (P*prtA*). Binding specificity was assessed by competition reactions in which increasing amounts (42, 85, 170, 340, 510, and 680 ng) of nonspecific (*nucA*; left) or specific (P*prtA*; right) unlabeled DNA template competed with labeled DNA for binding to CpxR-6×His. (B) EMSAs were performed using a nonlabeled PCR fragment containing P*prtA* and purified CpxR-6×His (at increasing amounts of 2.5, 5, 10, 20, or 40 pmol, as indicated) preincubated (+) or not preincubated (−) with 25 mM acetyl phosphate (AcP). (C) DNase I footprinting analysis was performed on coding and noncoding strands of the *prtA* promoter region. The DNA fragments were incubated with 0 (−) or 20 (+) pmol of purified CpxR-6×His. DNA ladder sequences (A, G, and T) are shown. The gels were sliced (noncontiguous lanes from a single gel are indicated by dashed lines) to exclude nonoptimal protein concentrations assayed or ladder lanes that resulted in smeared patterns. The nucleotide sequences of the CpxR-protected regions are indicated, and the protected DNA regions are underlined. A dotted line indicates the overlap of the protected sequences in each strand.

to the *prtA* translational ATG start site. This protected region overlapped the *in silico*-predicted CpxR consensus binding motif sequence (Fig. 3).

CpxR transcriptionally regulates PrtA expression in a temperature-dependent manner. In light of our results and to analyze CpxR influence on PrtA expression, a *cpxR* mutant strain was used and secreted proteolytic activity was assayed. At 30°C, the activity was not significantly affected by *cpxR* inactivation (Fig. 5A, left side of graph). However, at 37°C, a 40% increase in secreted proteolytic activity was obtained in the *cpxR* mutant strain compared to that in the wild-type strain (Fig. 5A, right side of graph). Complementation of *cpxR* inactivation in *trans* by expression of CpxR from the pBB5::*cpxR* plasmid restored the activity of the mutant strain to wild-type levels at 37°C, corroborating the *cpxR*-dependent phenotype. No significant differences were obtained at 30°C (Fig. 5A). These results were also reflected in the proteolytic halos detected when bacteria were grown in LB agar-skim milk plates (Fig. 5A, bottom). In agreement, the analysis of secreted protein profiles of the wild-type and *cpxR* strains by SDS-PAGE showed that only at 37°C was *cpxR* inactivation able to affect PrtA expression levels, being increased in the *cpxR* background (Fig. 5B). To verify that CpxR modulates PrtA expression at the transcriptional level, we measured fluorescence from wild-type and *cpxR* strains harboring the P*prtA-gfp* reporter plasmid. In good correlation with the results described above, inactivation of *cpxR* caused a 76% increase—in comparison with those of the wild-type strain—in fluorescence levels when bacteria were cultured at 37°C, while no significant difference was observed after growth at 30°C (Fig. 5C, left graph). In addition, *lipBCD* transcriptional activity was not influenced by *cpxR* inactivation (Fig. 5C, right graph). These results indicate that at 37°C, PrtA expression levels achieved in the *cpxR* strain are accomplished by derepression of *prtA* and not by variation in *lipBCD* expression. These results also indicate that thermal modulation of *lipBCD* transcriptional activity (as shown in Fig. 2C) might be under the control of a *cpxR*-independent mechanism.

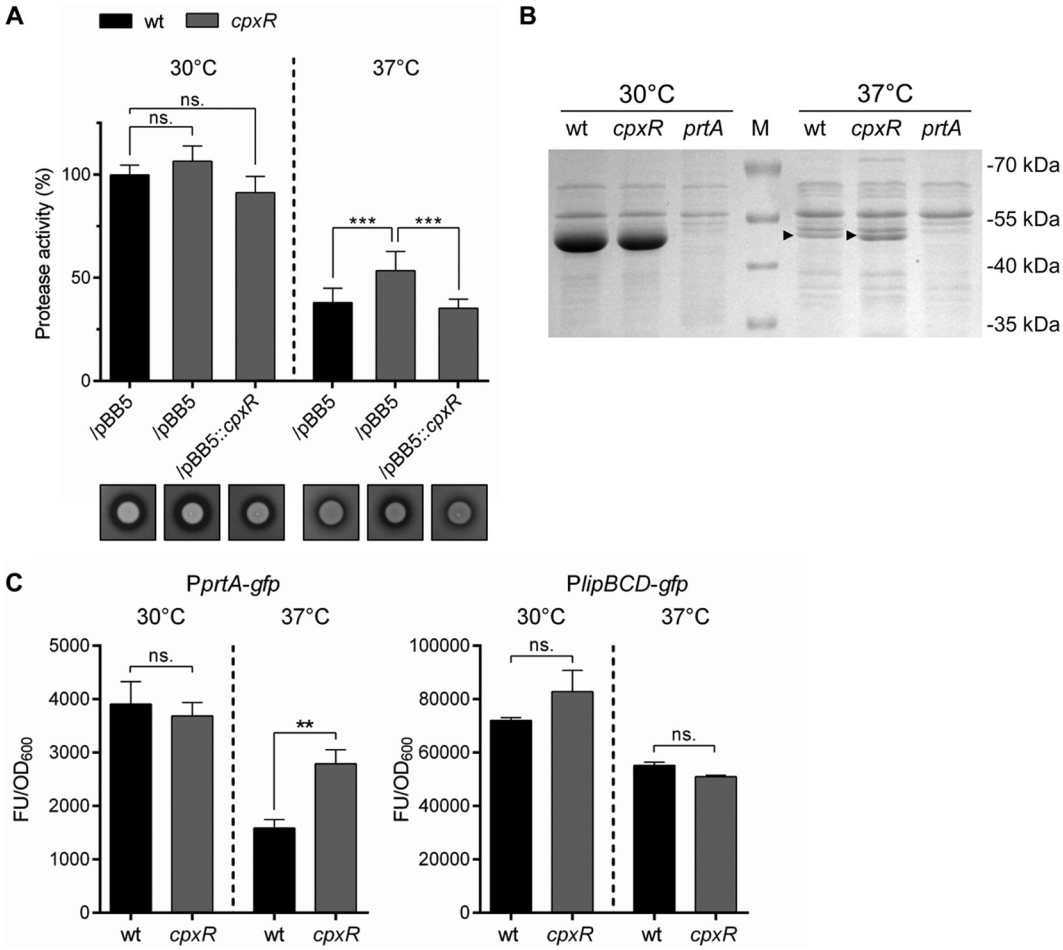

FIG 5 CpxR-dependent modulation of PrtA expression. (A) Secreted proteolytic activity from the wild-type or *cpxR* strains was measured by the azocaseinase assay. Results are expressed as percentages relative to the value obtained for the wt/pBB5 strain grown at 30°C. Below the graph, representative LB agar-skim milk plate images show protease degradation halos for each strain. Bacteria were grown for 16 h in LB medium supplemented with 15 μg/ml of gentamicin at the indicated temperatures. (B) SDS-PAGE analysis of extracellular proteins from wild-type and *cpxR* and *prtA* mutant strains, grown for 16 h at 30°C or 37°C. The arrowhead indicates the position of PrtA protein in the 37°C sample. Molecular mass standards are indicated to the right. (C) Transcriptional expression of *prtA* and *lipBCD*. Strains were grown in LB medium for 16 h at the indicated temperatures. Transcriptional activity was calculated as the ratio of GFP fluorescence and OD_{600} (FU/OD_{600}) measured from wild-type or *cpxR* strains carrying the P*prtA-gfp* or P*lipBCD-gfp* reporter plasmids. For panels A and C, means ± SDs from three independent experiments are shown. Significant differences by one-way ANOVA calculated with Bonferroni's multiple-comparison test are indicated as follows: ***, $P < 0.001$; **, $P < 0.01$; and ns., no significant difference.

Together, these results allow us to postulate a regulatory model for PrtA expression in which the CpxAR system is activated by temperature, being upregulated when bacteria are grown at 37°C. By direct interaction with the CpxR recognition motif located in the *prtA* promoter region, activated CpxR exerts a repressing action over *prtA* transcriptional activity.

Bacterial growth temperature defines the activity status of the *Serratia* CpxAR system. Our results indicate that CpxR-mediated repression over *prtA* is physiologically exerted at 37°C but not at 30°C, suggesting that the activity status of the CpxAR system is influenced by the bacterial growth temperature. Because there were no previous reports about the temperature impact on CpxAR system activity, and to further explore this phenotype, we examined by qRT-PCR the transcriptional level of *cpxP* from *Serratia* grown at 37°C or at 30°C. *cpxP* is a well-known member of the CpxAR regulon, which is transcriptionally activated by CpxR and is present in a group of *Enterobacteriaceae*, including *Salmonella*, *Yersinia*, and *Serratia* (41, 48). CpxP also serves as an auxiliary protein to regulate the CpxAR system in a negative-feedback loop by preventing autophosphorylation of CpxA through CpxP binding (28).

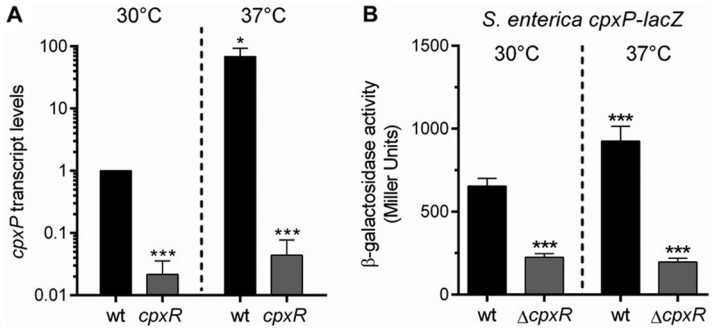

FIG 6 Growth temperature influences the activity status of the CpxAR system. (A) qRT-PCR analysis of *cpxP* expression. The wild-type and *cpxR* strains were grown in LB medium for 16 h at the indicated temperatures. Values obtained for the wild-type strain grown at 30°C were taken as the reference values. mRNA levels were normalized to the 16S rRNA gene, and relative expression was calculated using the $2^{-\Delta\Delta CT}$ method. Means ± SDs from three biological replicates are shown. Significant differences versus reference condition calculated by paired *t* test are indicated as follows: *, $P < 0.05$, and ***, $P < 0.001$. (B) β-Galactosidase activity from a *cpxP-lacZ* transcriptional fusions expressed in wild-type and Δ*cpxR Salmonella enterica* serovar Typhimurium 14028s strains. Bacterial cultures were grown in LB medium for 16 h at the indicated temperatures. Means ± SDs from three biological replicates are shown. Significant differences versus wild-type strain grown at 30°C by one-way ANOVA with Bonferroni's multiple-comparison test are indicated as follows: ***, $P < 0.001$.

As shown in Fig. 6A, transcriptional levels of *cpxP* increased 68-fold when *Serratia* was grown at 37°C compared to the values obtained at 30°C, while low expression levels could be detected in the *cpxR* background. This result reveals that the CpxAR-dependent induction over *cpxP* transcription is favored at 37°C, indicating that the *S. marcescens* CpxAR system is activated under this growth condition. In light of this result, we also determined *cpxP* transcriptional activity in a *Salmonella enterica* serovar Typhimurium 14028s strain that chromosomally harbors a *cpxP-lacZ* transcriptional reporter. Bacterial growth at 37°C mildly increased *Salmonella cpxP* expression in comparison with that at 30°C (Fig. 6B), suggesting that in addition to *S. marcescens*, temperature could be an environmental cue for CpxAR systems in other enterobacteria.

To further verify the regulatory action of the CpxAR system on PrtA expression, we also assayed a CpxAR-activating condition previously described for other enterobacteria. NlpE is an outer membrane lipoprotein that, when overexpressed, leads to CpxAR activation (27). Therefore, we transformed the *S. marcescens* strains with the pSU::*nlpE* expression plasmid and we measured proteolytic activity from the resultant strains grown either at 30°C or at 37°C. As shown in Fig. 7A, either by azocasein hydrolysis assay or by detection of proteolytic halos, NlpE overexpression resulted in a severe decrease of secreted proteolytic activity at both temperatures. At 30°C, NlpE-dependent repression was CpxR dependent, as we obtained a 63.5% reduction in the wild type but no significant effect in the *cpxR* strain, indicating that the inhibition is due to an activated CpxAR pathway. At 37°C, NlpE overexpression caused an 89.7% decrease in relation to the secreted proteolytic activity in the wild-type strain. However, we observed that NlpE overexpression also lowered proteolytic activity, by 51.7%, in the *cpxR* strain. In addition to potential CpxR-independent pathways that can be responsible for this last result, NlpE overexpression at 37°C caused a growth defect in all tested strains (Fig. 7B), indicating that at this temperature, NlpE expression also exerts a stressful, detrimental effect over *S. marcescens* growth capacity.

Together, our results allow us to propose that in *S. marcescens*, high temperature activates CpxAR signal transduction. This would result in increased levels of phosphorylated CpxR, a condition that enhances CpxR affinity for its recognition motif within *prtA* promoter. CpxAR system activation is also achieved by NlpE overexpression. Phospho-CpxR binding would result in repression of *prtA* transcription. In contrast, lower temperatures would decrease the levels of phosphorylated CpxR, leading to derepression of the transcriptional activity from the *prtA* promoter (Fig. 8 shows a scheme that depicts our working model). As shown in Fig. 5, in the absence of a

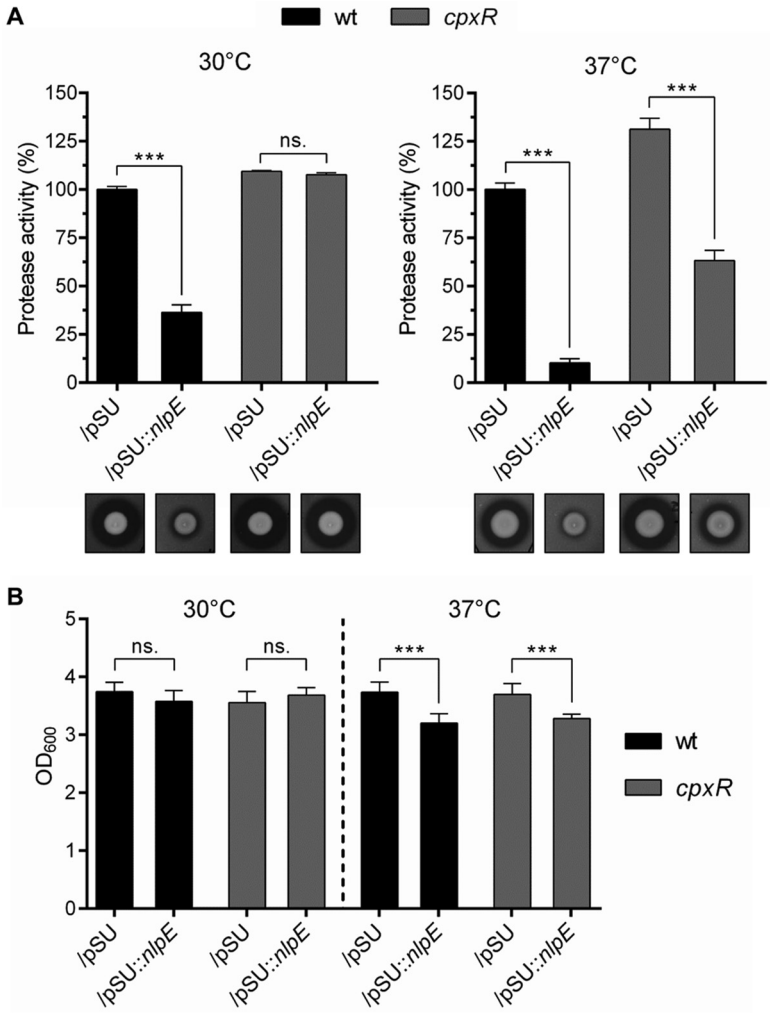

FIG 7 Effect of NlpE overexpression on CpxAR activation. (A) The indicated strains were grown in LB medium for 16 h at 30°C or 37°C. Secreted protease activity was measured by the azocaseinase assay. For each temperature, activity results are expressed as percentages relative to the value obtained for the wt/pSU strain. Below the graphs, representative LB agar-skim milk plate images show protease degradation halos for each strain. (B) Optical density from the bacterial cultures used for panel A was measured at 600 nm (OD_{600}). Means ± SDs from three independent experiments are shown. Significant differences in activity calculated by unpaired *t* test between the indicated strains are shown as follows: ***, $P < 0.001$, and ns., no significant difference.

CpxAR-inducing condition, overexpression of CpxR is not able compensate for the requirement of activated, phosphorylated CpxR to downregulate *prtA* expression.

PrtA expression influences *S. marcescens* biofilm formation capacity. *S. marcescens* displays biofilm formation capacity that has been shown to be related to its ability to colonize, persist, and proliferate on either biological or inert surfaces. *S. marcescens* biofilms form successfully on periodontal tissues (49), contact lenses (50), neonatal feeding tubes (51), and catheters, prostheses, and other medical devices (3, 6). *S. marcescens* also forms biofilms on corals (52, 53) and over zygomycete mycelium (54). More recently, the capacity of *S. marcescens* to generate mixed biofilms together with *Escherichia coli* and *Candida tropicalis* was correlated with the abundance of these three microorganisms in dysbiotic Crohn's disease patients (5). Taking into account that in other enterobacteria, the CpxAR pathway is involved in modulating the ability of biofilm generation (55–57), we examined whether PrtA could influence *S. marcescens* biofilm formation capacity.

To that aim, we performed *in vitro* biofilm assays in polystyrene microwell plates, followed by biofilm quantitation using crystal violet staining as detailed in Materials

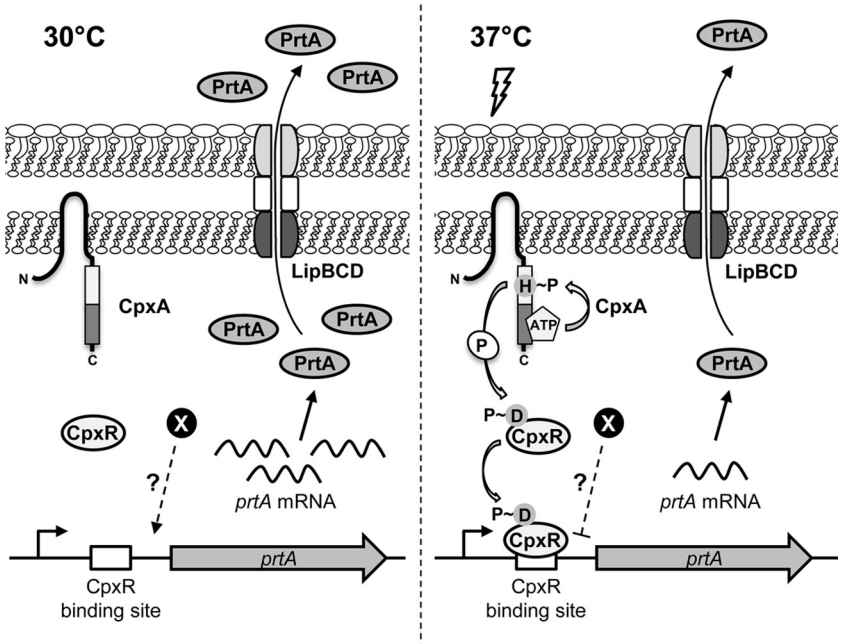

FIG 8 Proposed model for the regulation of PrtA expression. At 30°C (left), the CpxAR system is noninduced, yielding low levels of CpxR-P. High *prtA* transcript levels correlate with large amounts of PrtA detected in the extracellular space, and hence, high proteolytic activity levels are achieved. A growth temperature of 37°C (right) represents an inducing cue for CpxAR, increasing CpxR-P levels, which, in turn, repress PrtA expression by direct binding to *prtA* promoter region. PrtA expression decreases in comparison to that at 30°C. Still-uncovered regulatory mechanisms (represented by "X") might contribute to activate PrtA gene transcription at 30°C and/or repress its expression at 37°C.

and Methods. As shown in Fig. 9A, when the strains were grown at 30°C in either SLB medium (peptone at 10 g/liter and yeast extract at 5 g/liter)—a low-osmolarity condition that has been shown to enhance biofilm formation in other *Enterobacteriaceae* (57)—or LB medium, the lack of PrtA expression in the *prtA* strain reduced 56.9% or 38.2%, respectively, the capacity of the bacteria to form biofilm compared with that of the wild-type strain. In agreement with PrtA expression being downregulated at 37°C versus 30°C, *prtA* deficiency in biofilm formation was more attenuated at 37°C, showing a reduction of 30.2% in SLB medium or 31.2% in LB medium (Fig. 9A). Under all conditions, the *prtA* defective biofilm phenotype was restored to wild-type levels by PrtA expression in *trans* from the pBB2::*prtA* plasmid (Fig. 9A). These results demonstrate that PrtA expression contributes to the ability of *S. marcescens* to structure a biofilm community.

In addition, and in correlation with CpxR inhibitory action over PrtA expression at 37°C, *cpxR* inactivation enhanced 37.9% (in SLB medium) and 77.0% (in LB medium) the capacity of the wild-type strain to form biofilm at 37°C. In *trans* expression of CpxR from pBB5::*cpxR* reestablished the biofilm formation ability of the *cpxR* mutant to wild-type levels. As expected, at 30°C, *cpxR* inactivation did not show any effect on the biofilm phenotype when *S. marcescens* strains were grown either in LB medium or in SLB medium (Fig. 9B). This result reinforces the conclusion that CpxR-regulated PrtA expression is involved in *Serratia* biofilm development. Because we observed that PrtA expression was not associated with *S. marcescens* autolysis (data not shown) as was shown to be the case for secreted GelE metalloprotease in *Enterococcus faecalis* (58), we can discard the possibility that PrtA-dependent liberation of extracellular DNA could act as the modulator of the formation or maintenance of *S. marcescens* biofilm. A recent work by Selan and colleagues (59) showed that the *S. marcescens* ATCC 21074 PrtA homologue was able to impair the capacity of *Staphylococcus aureus* to attach to an inert matrix and develop biofilm. However, this ability was retained in a single-amino-acid-mutant protein that annuls the protease hydrolytic capacity, showing that the

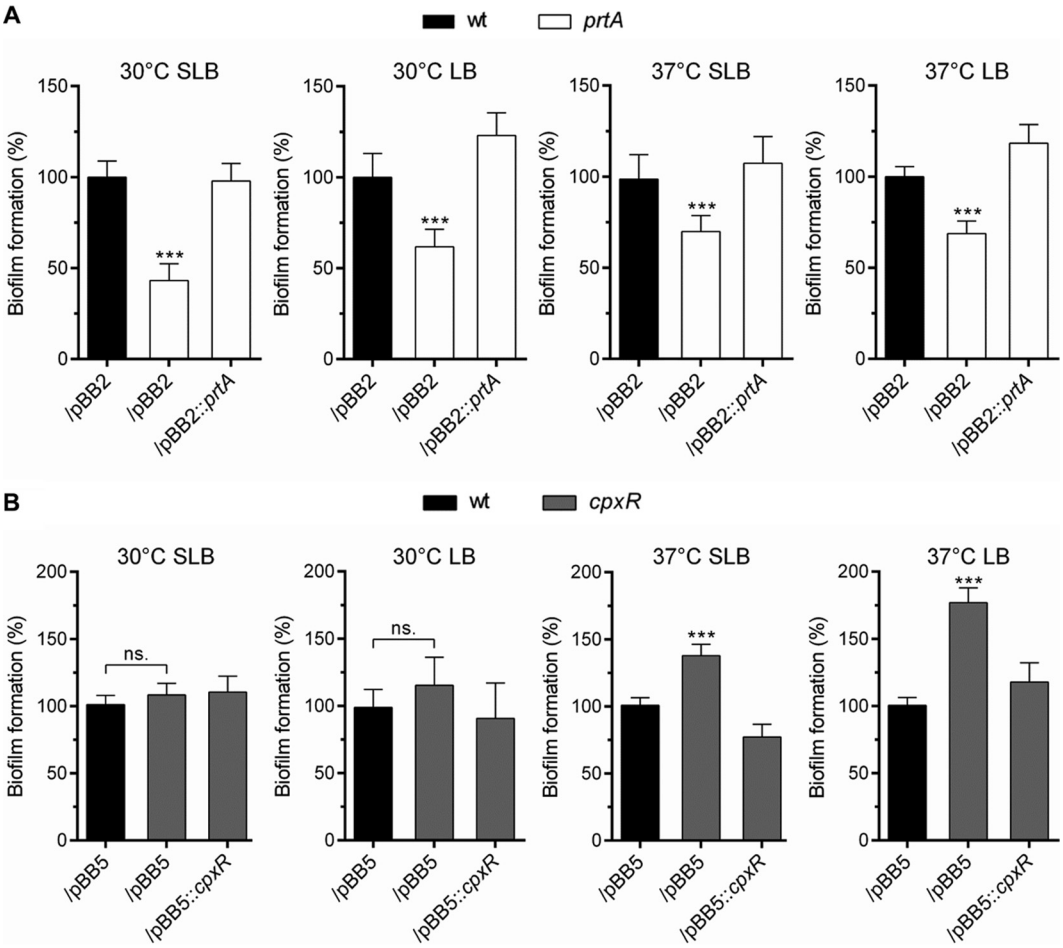

FIG 9 (A) PrtA involvement in *S. marcescens* biofilm phenotype; (B) CpxR influence on biofilm formation. Strains were grown in SLB or LB culture medium at 30 or 37°C for 48 h in 96-well microtiter plates. The adhered biofilm was measured by crystal violet staining. Results are expressed as percentages relative to the values obtained for the wt/pBB2 (A) or wt/pBB5 (B) strain. Means ± SDs from three independent experiments are shown. Significant differences in activity calculated by one-way ANOVA with Bonferroni's multiple-comparison test are indicated as follows: ***, $P < 0.001$, and ns., no significant difference.

biofilm interference phenotype was independent of the catalytic activity of the protein. Together with our results, these findings allow us to hypothesize alternative scenarios that are the object of our ongoing research: (i) PrtA can convert an inert substrate into a functional one that enhances biofilm formation, (ii) PrtA could favor *S. marcescens* biofilm formation by exerting its hydrolytic activity over a substrate that is detrimental for biofilm formation, or (iii) PrtA harbors structural properties that promote adherence of *S. marcescens* to the attachment surfaces or aid the stability of the extracellular matrix that allows cell-cell interactions in the biofilm assembly process.

Concluding remarks. We here show novel insights into the regulation of PrtA expression at the transcriptional level. An increase in PrtA expression in response to temperature decrease allows us to hypothesize that metalloprotease activity is required for the interaction with either the external ambient temperature or unregulated-body-temperature hosts. Downregulation of PrtA expression levels at 37°C would favor *Serratia* in the transition to mammalian niches. Thermoregulation would allow colonization of regulated-body-temperature hosts by limiting the cytotoxic capacity of PrtA toward mammalian cells (60). At this temperature, CpxR-dependent repression would strengthen PrtA downregulation in the presence of conditions related to CpxAR-mediated surface sensing or the detection of threats to bacterial envelope integrity.

We showed that involvement of PrtA in biofilm formation is not constrained by environmental temperature, which is indicative of a relevant role for this protein in the

capacity of *Serratia* to form multicellular communities in a diversity of extra- or intrahost niches. We have previously demonstrated that in *S. marcescens*, the biogenesis of outer membrane vesicles (OMVs) is thermoregulated and that PrtA forms part of OMV cargo (39). Like PrtA expression, OMV production is enhanced at temperatures below 30°C. Because it has been observed that OMVs can integrate bacterial biofilm structures (61), we can conjecture that PrtA could enhance bacterial community formation not only as a secreted soluble protein but also by exerting its action as a component of OMVs.

Previous findings showed that PrtA is able to breach host barriers or alter immune defenses: it was reported to be an agent capable for the hydrolysis of several host substrates, such as the Hageman factor/kallikrein-kinin coagulation system (62–65), the components of human complement (60), the heavy chains of IgG and IgA immunoglobulins (66), and the rip-trialysin antimicrobial peptide present in insect salivary fluids (67). Conceivably, PrtA displays a dual role as biofilm enhancer factor that, at the same time, leads to attainment of a localized threshold concentration efficacious to exert the enzymatic action over host components, facilitating colonization and invasion processes.

MATERIALS AND METHODS

Bacterial strains and plasmids. *Serratia marcescens* RM66262 is a nonpigmented clinical isolate from a patient with a urinary tract infection (41). The strains and plasmids used in this study are listed in Table 1.

Insertion mutations in *prtA* and *lipB* were constructed by cloning internal regions of each gene into pKNOCK suicide plasmids (68). For constructing the *prtA* strain, primers prtA left-Fw and prtA right-Rv were used to PCR amplify from the chromosome a 2,556-bp DNA region encompassing the *prtA* gene, which was subsequently cloned into pGEM-T. The resulting plasmid, pGEM-T::*prtA*, was afterwards digested with NotI and SmaI restriction enzymes to obtain an internal 560-bp region of *prtA*. For the *lipB* strain, an internal 621-bp region was PCR amplified from the chromosome and subsequently digested with BamHI and XhoI enzymes. These internal DNA fragments were purified and ligated into the respective sites of pKNOCK-Cm (*prtA* mutant) or pKNOCK-Gm (*lipB* mutant). The resulting plasmids were introduced into competent *E. coli* SM10 (λpir) cells by chemical transformation and then mobilized into the *S. marcescens* wild-type strain by conjugation. Insertional mutants were confirmed by PCR analysis.

To construct the pBBR1-MCS2::*prtA* plasmid, the *prtA* gene was amplified from the chromosome by PCR using primers prtA ATG-Fw and prtA-Rv. The 1,500-bp fragment obtained was purified and cloned into KpnI-HindIII-digested plasmid pBBR1-MCS2, and the resulting plasmid was mobilized into *S. marcescens prtA* by conjugation.

To analyze the transcriptional activity of *prtA*, the putative promoter region was PCR amplified from the chromosome using primers prom prtA-Fw and prom prtA-Rv and cloned into pGEM-T. Afterwards, pGEM-T::P*prtA* was digested with EcoRI enzyme, yielding a 443-bp fragment which was subsequently cloned into the same site of pPROBE-NT [ASV] *gfp*-reporter vector (69). To study *lipBCD* transcriptional expression, the promoter region of the operon was amplified by PCR using the primers prom lipBCD-Fw2 and prom lipBCD-Rv (Table 2). The purified PCR product was digested with the HindIII and XbaI restriction enzymes and was ligated into the same sites of pPROBE-OT (69). Either pPROBE::P*prtA-gfp* or pPROBE::P*lipBCD-gfp* was mobilized by conjugation into the *S. marcescens* wild-type or *cpxR* strain.

For the complementation of the *cpxR* mutant, the *cpxR* gene was first PCR amplified from the chromosome using primers cpxR-Fw and cpxR-Rv, and the DNA product was cloned into the pGEM-T vector. Then plasmid pGEM-T::*cpxR* was digested using BamHI and SacI enzymes, yielding a 764-bp fragment corresponding to the coding region of *cpxR*, which was purified and cloned into BamHI-SacI-digested pBBR1-MCS5. The plasmid was then mobilized into *S. marcescens cpxR* by conjugation.

Construction of the pSU36::*nlpE* plasmid was done by amplifying the coding region of *nlpE* from the chromosome with primers nlpE-Fw.SalI and nlpE-Rv.HindIII, yielding a 703-bp fragment which was subsequently purified, digested with SalI and HindIII enzymes, and cloned into previously SalI-HindIII-restricted pSU36. The construction was then introduced into the *S. marcescens* wild-type or *cpxR* strain by electroporation.

Media and growth conditions. Strains were routinely cultured in Miller's Luria-Bertani (LB) medium at the desired temperature. For biofilm assays, SLB medium (peptone at 10 g/liter and yeast extract at 5 g/liter) was also used. The antibiotics used for selection in *E. coli* or *S. marcescens* were tetracycline, chloramphenicol, kanamycin, and ampicillin at concentrations of 4, 20, 50, and 100 μg/ml, respectively.

Proteomic analysis. The excised band of interest was submitted to the CEQUIBIEM proteomic facility in Argentina. Mass spectrometric data were obtained using an Ultraflex II (Bruker) matrix-assisted laser desorption ionization–time of flight (MALDI-TOF)/TOF spectrometer. The resulting mass spectra were used for the identification of the protein by the Mascot search engine using the preliminary gene sequence of *S. marcescens* DB11 on the SEED server (http://www.theseed.org).

Protease assays. As a qualitative approach, 2 μl of overnight-grown cultures were inoculated on LB agar plates supplemented with skim milk at 2% (wt/vol) and incubated for 16 h at 30 or 37°C. Protease activity was identified as a distinct clearing of the milk around the colony. For quantitative analysis, protease activity (here called the azocaseinase assay) was measured from culture supernatants using

TABLE 1 Strains and plasmids used in this study

Strain or plasmid	Genotype and/or comments	Reference or source
Strains		
S. marcescens		
Wild type	RM66262; clinical isolate	41
prtA strain	*prtA*::pKNOCK-Cm	This work
lipB strain	*lipB*::pKNOCK-Gm	This work
cpxR strain	*cpxR*::pKNOCK-Cm	78
wt/pBB2	Wild type/pBBR1-MCS2 Km^r	76
prtA/pBB2 strain	*prtA*::pKNOCK-Cm/pBBR1-MCS2 Km^r	This work
prtA/pBB2::*prtA* strain	*prtA*::pKNOCK-Cm/pBBR1-MCS2::*prtA* Km^r	This work
wt/pBB5	Wild type/pBBR1-MCS5 Gm^r	This work
wt/P*prtA-gfp*	Wild type/pPROBE-NT [ASV]::P*prtA*	This work
cpxR/P*prtA-gfp* strain	*cpxR*/pPROBE-NT [ASV]::P*prtA*	This work
wt/P*lipBCD-gfp*	Wild type/pPROBE-OT::P*lipBCD*	This work
cpxR/P*lipBCD-gfp* strain	*cpxR*/pPROBE-OT::P*lipBCD*	This work
cpxR/pBB5 strain	*cpxR*::pKNOCK-Cm/pBBR1-MCS5 Gm^r	This work
cpxR/pBB5::*cpxR* strain	*cpxR*::pKNOCK-Cm/pBBR1-MCS5::*cpxR* Gm^r	This work
wt/pSU	Wild type/pSU36 Km^r	This work
wt/pSU::*nlpE*	Wild type/pSU36::*nlpE* Km^r	This work
cpxR/pSU strain	*cpxR*::pKNOCK-Cm/pSU36 Km^r	This work
cpxR/pSU::*nlpE* strain	*cpxR*::pKNOCK-Cm/pSU36::*nlpE* Km^r	This work
E. coli		
One Shot TOP10	F$^-$ *mcrA* Δ(*mrr-hsdRMS-mcrBC*) ϕ80*lacZ*ΔM15 Δ*lacX74 nupG recA1 araD139* Δ(*ara-leu*)*7697 galE15 galK16 rpsL endA1* Sm^r	Invitrogen
SM10 λpir	*thiJ thr leu tonA lacY 61lic recA*::RP4-2-Tc::Mu λpir Km^r	
M15/pRep4	F$^-$ ϕ80*lacZ*ΔM15 *thi lac mtl recA*$^+$ p*lacI* Km^r	Qiagen
Salmonella enterica serovar Typhimurium		
Wild type	14028s *cpxP-lacZ*	79
Δ*cpxR* strain	14028s Δ*cpxRA cpxP-lacZ*	80
Plasmids		
pGEM-T::*prtA*	PCR-amplified *prtA* coding sequence and flanking regions cloned in pGEM-T; Amp^r	This work
pBB2	pBBR1-MCS2 Km^r; broad host range	81
pBB2::*prtA*	pBBR1-MCS2::*prtA* Km^r	This work
pGEM-T::P*prtA*	PCR-amplified *prtA* promoter region cloned in pGEM-T; Amp^r	This work
P*prtA-gfp*	pPROBE-NT [ASV]::P*prtA*	This work
P*lipBCD-gfp*	pPROBE-OT::P*lipBCD*	This work
pGEM-T::*cpxR*	PCR-amplified *cpxR* coding sequence cloned in pGEM-T; Amp^r	This work
pBB5	pBBR1-MCS5 Gm^r; broad host range	81
pBB5::*cpxR*	pBBR1-MCS5::*cpxR* Gm^r	This work
pSU	pSU36 Km^r; derived from pACYC184	82
pSU::*nlpE*	pSU36::*nlpE*	This work
pQE32::*cpxR*	Expression vector for CpxR-6×His	This work

azocasein (Sigma) as a colorimetric substrate as previously described (42). Cultures were centrifuged and filtered to remove bacteria. A 50-μl aliquot of the filtered supernatant was mixed with 50 μl of 1% (wt/vol) azocasein and 140 μl of phosphate-buffered saline (PBS) and incubated for 1 h at 37°C. The reaction was stopped by addition of 80 μl of 10% (vol/vol) trichloroacetic acid, and the mixture was incubated for 15 min on ice. The tubes were centrifuged at 10,000 × *g* for 10 min. The clear supernatant was removed, and its absorbance at 340 nm (A_{340}) relative to that of a medium control was determined. This value was then normalized to the optical density at 600 nm (OD_{600}) from the original culture.

***β*-Galactosidase activity assays.** For β-galactosidase activity assays, bacteria were grown for 16 h in LB medium at 30 or 37°C, and the activity was determined as described previously (70).

RNA purification. Total RNA was extracted from stationary-phase cultures grown for 16 h in LB medium at 30 or 37°C. A total of 250 μl of ice-cold 5% (vol/vol) water-saturated phenol (pH 5.5) in ethanol was added to 1 ml of the cultures to stop the degradation of RNA. Cells were centrifuged at 6,000 × *g* for 5 min at 4°C and resuspended in 100 μl of 10 mM Tris-HCl and 1 mM EDTA (pH 8.0). The RNA extraction was performed using the Promega SV total RNA isolation kit, following the manufacturer's instructions.

qRT-PCR. cDNA synthesis was performed using random hexamers, 2 μg of total RNA, and 1 U of SuperScript II RNase H2 reverse transcriptase (Invitrogen). Five microliters of a 1/10 dilution of each cDNA was used as the template in quantitative real-time PCR (qRT-PCR) (reaction mixture, 20 μl), using primers prtA RT-Fw, prtA RT-Rv, cpxP RT-Fw, and cpxP RT-Rv. 16S rRNA was used as the reference gene. A 250-bp fragment was amplified in all cases. The reactions were carried out in the presence of the double-stranded-DNA-specific dye SYBR green (Molecular Probes) and monitored in real time with a Mastercyclerep Realplex real-time PCR system (Eppendorf). The relative expression was calculated using the

TABLE 2 Primers used in this study

Primer	Sequence (5′→3′)
prtA left-Fw	AGGCTCGCTGCCGTTAG
prtA right-Rv	CCTGATCGTGCGTTCGC
prtA ATG-Fw	GGGGTACCGTTATGTCTATCTGTCTG
prtA-Rv	CCCAAGCTTTTACACGATAAAGTCAGTG
lipB-Fw.BamHI	CGCGGATCCAAAGGCGATGCGGTATTGC
lipB-Rv.XhoI	CCGCTCGAGGAACGCGTTGACGTTGCC
cpxR-Fw	ACGGGATCCATATGAACAAGATTCTGTTAG
cpxR-Rv	AGCAAGCTTTCATGTTGCAGATACCATC
prom prtA-Fw	CGGAATTCAGGCTCGCCGCCGATAG
prom prtA-Rv	CGAAGCTTAACCTCCCCGTAAGCCAG
prom lipBCD-Fw2	CCCAAGCTTCCATAGCCGTGCCAGGAA
prom lipBCD-Rv	TGCTCTAGACCGCAATTTCATTGCGCG
16S RT-Fw	AAACTGGAGGAAGGTGGGGATGAC
16S RT-Rv	ATGGTGTGACGGGCGGTGTG
prtA RT-Fw	TTACCCGTGAGAACCAAACC
prtA RT-Rv	TGTAGTTGCCGAAGGTGATG
cpxP RT-Fw	TGGAAGCCATGCATAAACTG
cpxP RT-Rv	TACGCTGCTGATGTTTCTGG
nucA-Fw	GCTCTAGAGGCAAGACGCGCAACTGG
nucA-Rv	CCGCTCGAGGAAATCGGCGCCCTTCGG
nlpE-Fw.SalI	ACGCGTCGACCTATGAAAAAAATTACGGTAGC
nlpE-Rv.HindIII	AGCAAGCTTTTATTTGCTGCTGCAGTTC

threshold cycle (C_T) values obtained for each sample, as follows: relative expression $= 2^{-\Delta\Delta CT}$, with $\Delta C_T = C_{T\text{transcript of interest}} - C_{T16S}$ and $\Delta\Delta C_T = \Delta C_{T\text{experimental condition}} - \Delta C_{T\text{reference condition}}$. The average values were calculated from triplicate samples.

Construction, expression, and purification of CpxR-6×His. The *cpxR* gene was PCR amplified from *S. marcescens* RM66262 genomic DNA using primers cpxR-Fw and cpxR-Rv (Table 2) and cloned into a pQE32 vector as an N-terminal fusion to a 6×His tag. The fusion protein was expressed in *E. coli* M15/pRep4. Cells were grown in 300 ml of LB medium at 30°C to an OD_{600} of 0.6. Following induction with 50 μM isopropyl-β-D-thiogalactopyranoside (IPTG) and incubation for 16 h at 30°C, cells were harvested and disrupted by sonication. The CpxR-6×His protein was purified using an Ni^{2+}-nitrilotriacetic acid-agarose affinity chromatography column according to the QIAexpression purification protocol (Qiagen) and exhaustively dialyzed against 20 mM Tris-HCl (pH 7.4)–500 mM NaCl. The protein concentration was determined by a bicinchoninic acid assay (Sigma), and the protein profile of the purified CpxR-His6X protein was analyzed by SDS-PAGE.

Prediction of CpxR-binding site. The consensus motif for the CpxR-binding site was generated by training the Multiple Expectation Maximization for motif Elicitation (MEME) tool (46) using as input cognate binding sequences in the promoter regions of the following CpxR-regulated genes from *Salmonella*: *cpxP1*, *cpxP2*, *htrA*, *ppiA*, *yccA*, *spy*, *dsbA*, *amiA*, *amiC*, *cueP*, *gesA*, and *scsA* (71–75). The obtained matrix was then submitted to the Find Individual Motif Occurrences (FIMO) tool to detect the presence of the motif in the promoter region of the *prtA* gene from *S. marcescens* (47).

Protein-DNA interaction analysis. Electrophoretic gel mobility shift competition assays (EMSAs) and DNase I footprinting assays were performed using 14 fmol of a ^{32}P-labeled DNA fragment containing the *prtA* promoter (P*prtA*) and 20 pmol of purified CpxR-6×His protein following basically previously described protocols (76). Prior to addition of the DNA probe, CpxR-6×His protein was phosphorylated by incubation with 25 mM acetyl phosphate at 30°C for 30 min. The specificity of binding was assayed using the unlabeled P*prtA* probe or a 436-bp PCR fragment corresponding to the *nucA* gene from *S. marcescens* as a nonspecific competitor. The primers used to amplify the P*prtA* region and *nucA* are listed in Table 2. To evaluate the effect of CpxR phosphorylation upon binding, EMSAs were performed using 14 fmol of a nonlabeled DNA fragment containing the P*prtA* promoter and 2.5, 5, 10, 20, or 40 pmol of purified CpxR-6×His with or without previous incubation with 25 mM acetyl phosphate. DNase I protection assays were done for both DNA strands. The DNA sequence ladder was generated in parallel using the appropriate primers and the Sequenase DNA sequencing kit (Promega). After electrophoresis, the gels were either dried and exposed to autoradiography or stained with SYBR green (Invitrogen).

Biofilm assays. The quantification of biofilm production was performed by following a previously established protocol (77), with slight modifications. Briefly, in a 96-well microtiter plate, single colonies were inoculated into 150 μl of LB or SLB broth in sextuplicate and grown statically at the desired temperature for 48 h. The culture was aspirated, and wells were washed with water. Each well was stained with 0.5% crystal violet for 15 min at room temperature and then washed three times with water. The wells were allowed to dry for 1 h before 200 μl of ethanol-acetone (80:20) was added, and the plate was shaken at room temperature for 1 h to dissolve crystal violet from the well walls. Finally, absorbance at 562 nm was determined using a Synergy 2 plate reader (Biotek).

ACKNOWLEDGMENTS

We are grateful to Marina Avecilla for excellent technical assistance. We thank Silvana Boggio for the kind gift of azocaseine. We are grateful to Nicolas Figueroa for technical advice regarding biofilm assays.

E.G.V. and J.F.M. are Career Investigators of Consejo de Investigaciones Científicas y Tecnológicas (CONICET), Argentina. R.E.B., M.V.M., and M.L. have fellowships from CONICET. This work was supported by grants from Agencia Nacional de Promoción Científica y Tecnológica (ANPCyT), Argentina, PICT 2012-1403 and PICT 2016-1137, to E.G.V.

The funders had no role in study design, data collection and interpretation, or the decision to submit the work for publication.

REFERENCES

1. Gastmeier P. 2014. Serratia marcescens: an outbreak experience. Front Microbiol 5:81. https://doi.org/10.3389/fmicb.2014.00081.
2. Grimont PA, Grimont F. 1978. The genus Serratia. Annu Rev Microbiol 32:221–248.
3. Mahlen SD. 2011. Serratia infections: from military experiments to current practice. Clin Microbiol Rev 24:755–791. https://doi.org/10.1128/CMR.00017-11.
4. Lawe-Davies O, Bennett S. 2017. WHO publishes list of bacteria for which new antibiotics are urgently needed. News release. WHO, Geneva, Switzerland. http://www.who.int/mediacentre/news/releases/2017/bacteria-antibiotics-needed/en/.
5. Hoarau G, Mukherjee PK, Gower-Rousseau C, Hager C, Chandra J, Retuerto MA, Neut C, Vermeire S, Clemente J, Colombel JF, Fujioka H, Poulain D, Sendid B, Ghannoum MA. 2016. Bacteriome and mycobiome interactions underscore microbial dysbiosis in familial Crohn's disease. mBio 7:e01250-16. https://doi.org/10.1128/mBio.01250-16.
6. Petersen LM, Tisa LS. 2013. Friend or foe? A review of the mechanisms that drive Serratia towards diverse lifestyles. Can J Microbiol 59:627–640.
7. Nakahama K, Yoshimura K, Marumoto R, Kikuchi M, Lee IS, Hase T, Matsubara H. 1986. Cloning and sequencing of Serratia protease gene. Nucleic Acids Res 14:5843–5855. https://doi.org/10.1093/nar/14.14.5843.
8. Zhang L, Morrison AJ, Thibodeau PH. 2015. Interdomain contacts and the stability of serralysin protease from Serratia marcescens. PLoS One 10:e0138419. https://doi.org/10.1371/journal.pone.0138419.
9. Akatsuka H, Binet R, Kawai E, Wandersman C, Omori K. 1997. Lipase secretion by bacterial hybrid ATP-binding cassette exporters: molecular recognition of the LipBCD, PrtDEF, and HasDEF exporters. J Bacteriol 179:4754–4760. https://doi.org/10.1128/jb.179.15.4754-4760.1997.
10. Akatsuka H, Kawai E, Omori K, Shibatani T. 1995. The three genes lipB, lipC, and lipD involved in the extracellular secretion of the Serratia marcescens lipase which lacks an N-terminal signal peptide. J Bacteriol 177:6381–6389. https://doi.org/10.1128/jb.177.22.6381-6389.1995.
11. Ishii K, Adachi T, Hamamoto H, Sekimizu K. 2014. Serratia marcescens suppresses host cellular immunity via the production of an adhesion-inhibitory factor against immunosurveillance cells. J Biol Chem 289:5876–5888. https://doi.org/10.1074/jbc.M113.544536.
12. Ishii K, Adachi T, Hara T, Hamamoto H, Sekimizu K. 2014. Identification of a Serratia marcescens virulence factor that promotes hemolymph bleeding in the silkworm, Bombyx mori. J Invertebr Pathol 117:61–67. https://doi.org/10.1016/j.jip.2014.02.001.
13. Kreger AS, Lyerly DM, Hazlett LD, Berk RS. 1986. Immunization against experimental Pseudomonas aeruginosa and Serratia marcescens keratitis. Vaccination with lipopolysaccharide endotoxins and proteases. Invest Ophthalmol Vis Sci 27:932–939.
14. Kurz CL, Chauvet S, Andres E, Aurouze M, Vallet I, Michel GP, Uh M, Celli J, Filloux A, De Bentzmann S, Steinmetz I, Hoffmann JA, Finlay BB, Gorvel JP, Ferrandon D, Ewbank JJ. 2003. Virulence factors of the human opportunistic pathogen Serratia marcescens identified by in vivo screening. EMBO J 22:1451–1460. https://doi.org/10.1093/emboj/cdg159.
15. Lyerly D, Kreger A. 1979. Purification and characterization of a Serratia marcescens metalloprotease. Infect Immun 24:411–421.
16. Lyerly DM, Kreger AS. 1983. Importance of Serratia protease in the pathogenesis of experimental Serratia marcescens pneumonia. Infect Immun 40:113–119.
17. Pineda-Castellanos ML, Rodriguez-Segura Z, Villalobos FJ, Hernandez L, Lina L, Nunez-Valdez ME. 2015. Pathogenicity of isolates of Serratia marcescens towards larvae of the scarab Phyllophaga blanchardi (Coleoptera). Pathogens 4:210–228. https://doi.org/10.3390/pathogens4020210.
18. Taneja K, Bajaj BK, Kumar S, Dilbaghi N. 2017. Production, purification and characterization of fibrinolytic enzyme from Serratia sp. KG-2-1 using optimized media. 3 Biotech 7:184.
19. Suh Y, Benedik MJ. 1992. Production of active Serratia marcescens metalloprotease from Escherichia coli by alpha-hemolysin HlyB and HlyD. J Bacteriol 174:2361–2366. https://doi.org/10.1128/jb.174.7.2361-2366.1992.
20. Salamone PR, Wodzinski RJ. 1997. Production, purification and characterization of a 50-kDa extracellular metalloprotease from Serratia marcescens. Appl Microbiol Biotechnol 48:317–324. https://doi.org/10.1007/s002530051056.
21. Pansuriya RC, Singhal RS. 2010. Evolutionary operation (EVOP) to optimize whey independent serratiopeptidase production from Serratia marcescens NRRL B-23112. J Microbiol Biotechnol 20:950–957. https://doi.org/10.4014/jmb.0911.11023.
22. Aiyappa PS, Harris JO. 1976. The extracellular metalloprotease of Serratia marcescens. I. Purification and characterization. Mol Cell Biochem 13:95–100. https://doi.org/10.1007/BF01837059.
23. Bhagat S, Agarwal M, Roy V. 2013. Serratiopeptidase: a systematic review of the existing evidence. Int J Surg 11:209–217. https://doi.org/10.1016/j.ijsu.2013.01.010.
24. Danese PN, Silhavy TJ. 1997. The sigma(E) and the Cpx signal transduction systems control the synthesis of periplasmic protein-folding enzymes in Escherichia coli. Genes Dev 11:1183–1193. https://doi.org/10.1101/gad.11.9.1183.
25. Danese PN, Snyder WB, Cosma CL, Davis LJ, Silhavy TJ. 1995. The Cpx two-component signal transduction pathway of Escherichia coli regulates transcription of the gene specifying the stress-inducible periplasmic protease, DegP. Genes Dev 9:387–398. https://doi.org/10.1101/gad.9.4.387.
26. Nakayama S, Watanabe H. 1995. Involvement of cpxA, a sensor of a two-component regulatory system, in the pH-dependent regulation of expression of Shigella sonnei virF gene. J Bacteriol 177:5062–5069. https://doi.org/10.1128/jb.177.17.5062-5069.1995.
27. Snyder WB, Davis LJ, Danese PN, Cosma CL, Silhavy TJ. 1995. Overproduction of NlpE, a new outer membrane lipoprotein, suppresses the toxicity of periplasmic LacZ by activation of the Cpx signal transduction pathway. J Bacteriol 177:4216–4223. https://doi.org/10.1128/jb.177.15.4216-4223.1995.
28. DiGiuseppe PA, Silhavy TJ. 2003. Signal detection and target gene induction by the CpxRA two-component system. J Bacteriol 185:2432–2440. https://doi.org/10.1128/JB.185.8.2432-2440.2003.
29. Kurabayashi K, Hirakawa Y, Tanimoto K, Tomita H, Hirakawa H. 2014. Role of the CpxAR two-component signal transduction system in control of fosfomycin resistance and carbon substrate uptake. J Bacteriol 196:248–256. https://doi.org/10.1128/JB.01151-13.
30. Srinivasan VB, Vaidyanathan V, Mondal A, Rajamohan G. 2012. Role of the two component signal transduction system CpxAR in conferring cefepime and chloramphenicol resistance in Klebsiella pneumoniae NTUH-K2044. PLoS One 7:e33777. https://doi.org/10.1371/journal.pone.0033777.

31. Labbate M, Queck SY, Koh KS, Rice SA, Givskov M, Kjelleberg S. 2004. Quorum sensing-controlled biofilm development in Serratia liquefaciens MG1. J Bacteriol 186:692–698. https://doi.org/10.1128/JB.186.3.692-698.2004.
32. Rice SA, Koh KS, Queck SY, Labbate M, Lam KW, Kjelleberg S. 2005. Biofilm formation and sloughing in Serratia marcescens are controlled by quorum sensing and nutrient cues. J Bacteriol 187:3477–3485. https://doi.org/10.1128/JB.187.10.3477-3485.2005.
33. Labbate M, Zhu H, Thung L, Bandara R, Larsen MR, Willcox MD, Givskov M, Rice SA, Kjelleberg S. 2007. Quorum-sensing regulation of adhesion in Serratia marcescens MG1 is surface dependent. J Bacteriol 189:2702–2711. https://doi.org/10.1128/JB.01582-06.
34. Van Houdt R, Givskov M, Michiels CW. 2007. Quorum sensing in Serratia. FEMS Microbiol Rev 31:407–424. https://doi.org/10.1111/j.1574-6976.2007.00071.x.
35. Choe HS, Son SW, Choi HA, Kim HJ, Ahn SG, Bang JH, Lee SJ, Lee JY, Cho YH, Lee SS. 2012. Analysis of the distribution of bacteria within urinary catheter biofilms using four different molecular techniques. Am J Infect Control 40:e249–e254. https://doi.org/10.1016/j.ajic.2012.05.010.
36. Ray C, Shenoy AT, Orihuela CJ, Gonzalez-Juarbe N. 2017. Killing of Serratia marcescens biofilms with chloramphenicol. Ann Clin Microbiol Antimicrob 16:19. https://doi.org/10.1186/s12941-017-0192-2.
37. Castelli ME, Fedrigo GV, Clementin AL, Ielmini MV, Feldman MF, Garcia Vescovi E. 2008. Enterobacterial common antigen integrity is a checkpoint for flagellar biogenesis in Serratia marcescens. J Bacteriol 190:213–220. https://doi.org/10.1128/JB.01348-07.
38. Petersen LM, Tisa LS. 2012. Influence of temperature on the physiology and virulence of the insect pathogen Serratia sp. strain SCBI. Appl Environ Microbiol 78:8840–8844. https://doi.org/10.1128/AEM.02580-12.
39. McMahon KJ, Castelli ME, Garcia VE, Feldman MF. 2012. Biogenesis of outer membrane vesicles in Serratia marcescens is thermoregulated and can be induced by activation of the Rcs phosphorelay system 7. J Bacteriol 194:3241–3249. https://doi.org/10.1128/JB.00016-12.
40. Petersen LM, Tisa LS. 2014. Molecular characterization of protease activity in Serratia sp. strain SCBI and its importance in cytotoxicity and virulence. J Bacteriol 196:3923–3936. https://doi.org/10.1128/JB.01908-14.
41. Bruna RE, Revale S, Garcia Vescovi E, Mariscotti JF. 2015. Draft whole-genome sequence of Serratia marcescens strain RM66262, isolated from a patient with a urinary tract infection. Genome Announc 3(6):e01423-15. https://doi.org/10.1128/genomeA.01423-15.
42. Banno Y, Nozawa Y. 1982. Changes in particulate-bound protease activity during cold acclimation in Tetrahymena pyriformis. Biochim Biophys Acta 719:74–80. https://doi.org/10.1016/0304-4165(82)90309-9.
43. Marty KB, Williams CL, Guynn LJ, Benedik MJ, Blanke SR. 2002. Characterization of a cytotoxic factor in culture filtrates of Serratia marcescens. Infect Immun 70:1121–1128. https://doi.org/10.1128/IAI.70.3.1121-1128.2002.
44. Shanks RM, Stella NA, Hunt KM, Brothers KM, Zhang L, Thibodeau PH. 2015. Identification of SlpB, a cytotoxic protease from Serratia marcescens. Infect Immun 83:2907–2916. https://doi.org/10.1128/IAI.03096-14.
45. Stella NA, Callaghan JD, Zhang L, Brothers KM, Kowalski RP, Huang JJ, Thibodeau PH, Shanks RMQ. 2017. SlpE is a calcium-dependent cytotoxic metalloprotease associated with clinical isolates of Serratia marcescens. Res Microbiol https://doi.org/10.1016/j.resmic.2017.03.006.
46. Bailey TL, Gribskov M. 1998. Methods and statistics for combining motif match scores. J Comput Biol 5:211–221. https://doi.org/10.1089/cmb.1998.5.211.
47. Grant CE, Bailey TL, Noble WS. 2011. FIMO: scanning for occurrences of a given motif. Bioinformatics 27:1017–1018. https://doi.org/10.1093/bioinformatics/btr064.
48. Huang YH, Ferrieres L, Clarke DJ. 2009. Comparative functional analysis of the RcsC sensor kinase from different Enterobacteriaceae. FEMS Microbiol Lett 293:248–254. https://doi.org/10.1111/j.1574-6968.2009.01543.x.
49. Vieira Colombo AP, Magalhaes CB, Hartenbach FA, Martins do Souto R, Maciel da Silva-Boghossian C. 2016. Periodontal-disease-associated biofilm: a reservoir for pathogens of medical importance. Microb Pathog 94:27–34. https://doi.org/10.1016/j.micpath.2015.09.009.
50. Hinojosa JA, Patel NB, Zhu M, Robertson DM. 2017. Antimicrobial efficacy of contact lens care solutions against neutrophil-enhanced bacterial biofilms. Transl Vis Sci Technol 6:11. https://doi.org/10.1167/tvst.6.2.11.
51. Juma NA, Forsythe SJ. 2015. Microbial biofilm development on neonatal enteral feeding tubes. Adv Exp Med Biol 830:113–121. https://doi.org/10.1007/978-3-319-11038-7_7.
52. Alagely A, Krediet CJ, Ritchie KB, Teplitski M. 2011. Signaling-mediated cross-talk modulates swarming and biofilm formation in a coral pathogen Serratia marcescens. ISME J 5:1609–1620. https://doi.org/10.1038/ismej.2011.45.
53. Krediet CJ, Carpinone EM, Ritchie KB, Teplitski M. 2013. Characterization of the gacA-dependent surface and coral mucus colonization by an opportunistic coral pathogen Serratia marcescens PDL100. FEMS Microbiol Ecol 84:290–301. https://doi.org/10.1111/1574-6941.12064.
54. Hover T, Maya T, Ron S, Sandovsky H, Shadkchan Y, Kijner N, Mitiagin Y, Fichtman B, Harel A, Shanks RM, Bruna RE, Garcia-Vescovi E, Osherov N. 2016. Mechanisms of bacterial (Serratia marcescens) attachment to, migration along, and killing of fungal hyphae. Appl Environ Microbiol 82:2585–2594. https://doi.org/10.1128/AEM.04070-15.
55. Dorel C, Vidal O, Prigent-Combaret C, Vallet I, Lejeune P. 1999. Involvement of the Cpx signal transduction pathway of E. coli in biofilm formation. FEMS Microbiol Lett 178:169–175. https://doi.org/10.1111/j.1574-6968.1999.tb13774.x.
56. Dudin O, Geiselmann J, Ogasawara H, Ishihama A, Lacour S. 2014. Repression of flagellar genes in exponential phase by CsgD and CpxR, two crucial modulators of Escherichia coli biofilm formation. J Bacteriol 196:707–715. https://doi.org/10.1128/JB.00938-13.
57. Prigent-Combaret C, Brombacher E, Vidal O, Ambert A, Lejeune P, Landini P, Dorel C. 2001. Complex regulatory network controls initial adhesion and biofilm formation in Escherichia coli via regulation of the csgD gene. J Bacteriol 183:7213–7223. https://doi.org/10.1128/JB.183.24.7213-7223.2001.
58. Thomas VC, Thurlow LR, Boyle D, Hancock LE. 2008. Regulation of autolysis-dependent extracellular DNA release by Enterococcus faecalis extracellular proteases influences biofilm development. J Bacteriol 190:5690–5698. https://doi.org/10.1128/JB.00314-08.
59. Selan L, Papa R, Tilotta M, Vrenna G, Carpentieri A, Amoresano A, Pucci P, Artini M. 2015. Serratiopeptidase: a well-known metalloprotease with a new non-proteolytic activity against S. aureus biofilm. BMC Microbiol 15:207. https://doi.org/10.1186/s12866-015-0548-8.
60. Molla A, Matsumoto K, Oyamada I, Katsuki T, Maeda H. 1986. Degradation of protease inhibitors, immunoglobulins, and other serum proteins by Serratia protease and its toxicity to fibroblast in culture. Infect Immun 53:522–529.
61. Wang W, Chanda W, Zhong M. 2015. The relationship between biofilm and outer membrane vesicles: a novel therapy overview. FEMS Microbiol Lett 362:fnv117. https://doi.org/10.1093/femsle/fnv117.
62. Kamata R, Matsumoto K, Okamura R, Yamamoto T, Maeda H. 1985. The serratial 56K protease as a major pathogenic factor in serratial keratitis. Clinical and experimental study. Ophthalmology 92:1452–1459.
63. Kamata R, Yamamoto T, Matsumoto K, Maeda H. 1985. A serratial protease causes vascular permeability reaction by activation of the Hageman factor-dependent pathway in guinea pigs. Infect Immun 48:747–753.
64. Matsumoto K, Yamamoto T, Kamata R, Maeda H. 1984. Pathogenesis of serratial infection: activation of the Hageman factor-prekallikrein cascade by serratial protease. J Biochem 96:739–749.
65. Matsumoto K, Yamamoto T, Kamata R, Maeda H. 1986. Enhancement of vascular permeability upon serratial infection: activation of Hageman factor-kallikrein-kinin cascade. Adv Exp Med Biol 198(Part B):71–78.
66. Molla A, Kagimoto T, Maeda H. 1988. Cleavage of immunoglobulin G (IgG) and IgA around the hinge region by proteases from Serratia marcescens. Infect Immun 56:916–920.
67. Lee DJ, Lee JB, Jang HA, Ferrandon D, Lee BL. 2017. An antimicrobial protein of the Riptortus pedestris salivary gland was cleaved by a virulence factor of Serratia marcescens. Dev Comp Immunol 67:427–433. https://doi.org/10.1016/j.dci.2016.08.009.
68. Alexeyev MF. 1999. The pKNOCK series of broad-host-range mobilizable suicide vectors for gene knockout and targeted DNA insertion into the chromosome of gram-negative bacteria. Biotechniques 26:824–826, 828.
69. Miller WG, Leveau JH, Lindow SE. 2000. Improved gfp and inaZ broad-host-range promoter-probe vectors. Mol Plant Microbe Interact 13:1243–1250. https://doi.org/10.1094/MPMI.2000.13.11.1243.
70. Barchiesi J, Castelli ME, Di Venanzio G, Colombo MI, Garcia Vescovi E. 2012. The PhoP/PhoQ system and its role in Serratia marcescens pathogenesis. J Bacteriol 194:2949–2961. https://doi.org/10.1128/JB.06820-11.
71. Cerminati S, Giri GF, Mendoza JI, Soncini FC, Checa SK. 2017. The CpxR/CpxA system contributes to Salmonella gold-resistance by con-

trolling the GolS-dependent gesABC transcription. Environ Microbiol https://doi.org/10.1111/1462-2920.13837.
72. Pogliano J, Lynch AS, Belin D, Lin EC, Beckwith J. 1997. Regulation of Escherichia coli cell envelope proteins involved in protein folding and degradation by the Cpx two-component system. Genes Dev 11: 1169–1182.
73. Rico-Pérez G, Pezza A, Pucciarelli MG, de Pedro MA, Soncini FC, Garcia-del Portillo F. 2016. A novel peptidoglycan D,L-endopeptidase induced by Salmonella inside eukaryotic cells contributes to virulence. Mol Microbiol 99:546–556. https://doi.org/10.1111/mmi.13248.
74. Weatherspoon-Griffin N, Zhao G, Kong W, Kong Y, Morigen Andrews-Polymenis H, McClelland M, Shi Y. 2011. The CpxR/CpxA two-component system up-regulates two Tat-dependent peptidoglycan amidases to confer bacterial resistance to antimicrobial peptide. J Biol Chem 286: 5529–5539. https://doi.org/10.1074/jbc.M110.200352.
75. Yamamoto K, Ishihama A. 2006. Characterization of copper-inducible promoters regulated by CpxA/CpxR in Escherichia coli. Biosci Biotechnol Biochem 70:1688–1695. https://doi.org/10.1271/bbb.60024.
76. Di Venanzio G, Stepanenko TM, Garcia Vescovi E. 2014. Serratia marcescens ShlA pore-forming toxin is responsible for early induction of autophagy in host cells and is transcriptionally regulated by RcsB. Infect Immun 82:3542–3554. https://doi.org/10.1128/IAI.01682-14.
77. Pratt LA, Kolter R. 1998. Genetic analysis of Escherichia coli biofilm formation: roles of flagella, motility, chemotaxis and type I pili. Mol Microbiol 30:285–293.
78. Lazzaro M, Feldman MF, Garcia Vescovi E. 2017. A transcriptional regulatory mechanism finely tunes the firing of type VI secretion system in response to bacterial enemies. mBio 8:e00559-17. https://doi.org/10.1128/mBio.00559-17.
79. Pezza A, Pontel LB, Lopez C, Soncini FC. 2016. Compartment and signal-specific codependence in the transcriptional control of Salmonella periplasmic copper homeostasis. Proc Natl Acad Sci U S A 113:11573–11578. https://doi.org/10.1073/pnas.1603192113.
80. Cerminati S, Giri GF, Mendoza JI, Soncini FC, Checa SK. 2017. The CpxR/CpxA system contributes to Salmonella gold-resistance by controlling the GolS-dependent gesABC transcription. Environ Microbiol 19: 4035–4044. https://doi.org/10.1111/1462-2920.13837.
81. Kovach ME, Elzer PH, Hill DS, Robertson GT, Farris MA, Roop RM, II, Peterson KM. 1995. Four new derivatives of the broad-host-range cloning vector pBBR1MCS, carrying different antibiotic-resistance cassettes. Gene 166:175–176.
82. Bartolomé B, Jubete Y, Martinez E, de la Cruz F. 1991. Construction and properties of a family of pACYC184-derived cloning vectors compatible with pBR322 and its derivatives. Gene 102:75–78.